The Gammon Ferruginous Member: its chemostratigraphy, paleontology and mineral potential

J.D. Bamburak, T. Martins, M.P.B. Nicolas and X.M. Yang

Introduction

The discovery of anomalous rare-earth element (REE) concentrations in the Gammon Ferruginous Member of the Upper Cretaceous Pierre Shale (Bamburak et al., 2013) resulted from bulk inorganic geochemical profiling of the Cretaceous shale sequence in 2009 (Bamburak and Nicolas, 2009). Since that initial discovery, investigation of its REE potential has been carried out yearly to assess its source and economic potential (e.g. Bamburak and Nicolas, 2009; Bamburak et al., 2012).

Rare-earth element mineralization can be found in different types of deposits, including carbonatite, hydrothermal/magmatic Fe-REE, placer accumulations of heavy mineral assemblages, alkaline and peralkaline related, and ion-adsorption deposits (residual deposits of REE-bearing clays). Since the REE anomaly in the Gammon Ferruginous Member was in a clastic sedimentary sequence, the placer accumulation or ion-adsorption deposits were the best models to follow for further investigation. Bamburak et al. (2013) had concluded that the ion-adsorption deposit was unlikely. In this poster, the placer accumulation of heavy mineral assemblage model will be tested.

The Gammon Ferruginous Member outcrops at several sites in southwestern Manitoba and northeastern North Dakota. The detailed stratigraphy of the Gammon Ferruginous Member was described by Bamburak and Nicolas (2010) and Bamburak et al. (2012). This poster updates work carried out by the MGS during the past year on samples collected at the Spencer's ditch site (Figure 1) in southwestern Manitoba. The objectives were to characterize the REE mineralogy of the Gammon Ferruginous Member and to determine the nature and composition of potential REE hosts.

Background information and previous work

The Gammon Ferruginous Member of the Pierre Shale was named by Rubey (1930) for the numerous red-weathered ferruginous or sideritic concretions contained in the uniform, dark grey mudstone or silty shale occurring along Gammon Creek, on the northwest flank of the Black Hills in Wyoming. Until 1970, the presence of the Gammon Ferruginous Member was not known in Manitoba. However, Bannatyne (1970) recognized up to 54.9 m of Gammon Ferruginous Member in hundreds of oilwells in southwestern Manitoba. It occurred in the subsurface between calcareous speckled shale at the top of the Boyne Member of the Carlile Formation and the interbedded bentonite and black shale beds at the base of the Pembina Member of the Pierre Shale (Figure 2). The Gammon Ferruginous Member is equivalent to the Milk River Formation of Saskatchewan (Christopher and Yurkowski, 2007; Nicolas, 2009).

Of all of the known sites of Gammon Ferruginous Member in southwestern Manitoba, the Spencer's ditch locality in L.S. 15, Sec. 31, Twp. 3, Rge. 6, W 1st Mer. (Figure 1) has the highest relative REE values, as noted by Bamburak and Nicolas (2010a, b), Bamburak et al. (2012, 2013, 2014).

From a sample collected at the site, it was determined by portable X-ray fluorescence unit that the middle bed (sample 99-12-SD-002B) contained anomalous REE values. The major components are Al_2O_3, CaO, Fe_2O_3 and SiO_2.

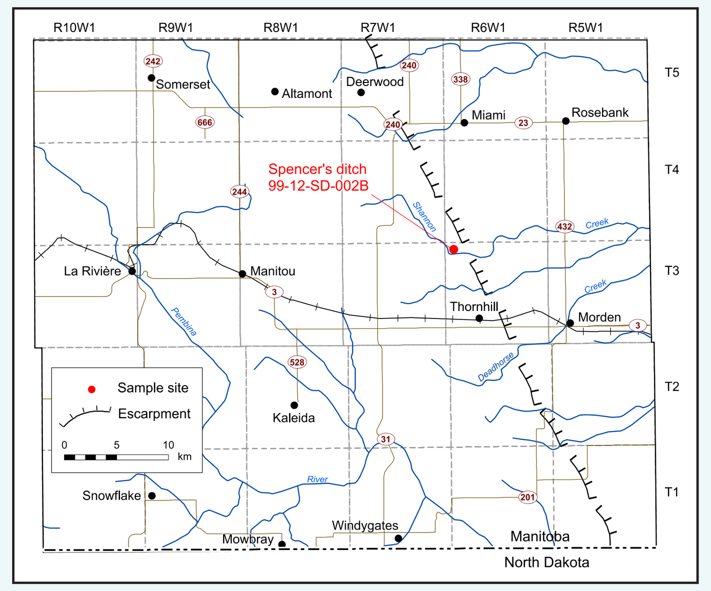

Figure 1: Location of Gammon Ferruginous Member sample 99-12-SD-002B collected at the Spencer's ditch site in the Pembina Hills area of southwestern Manitoba (Bamburak et al. 2012).

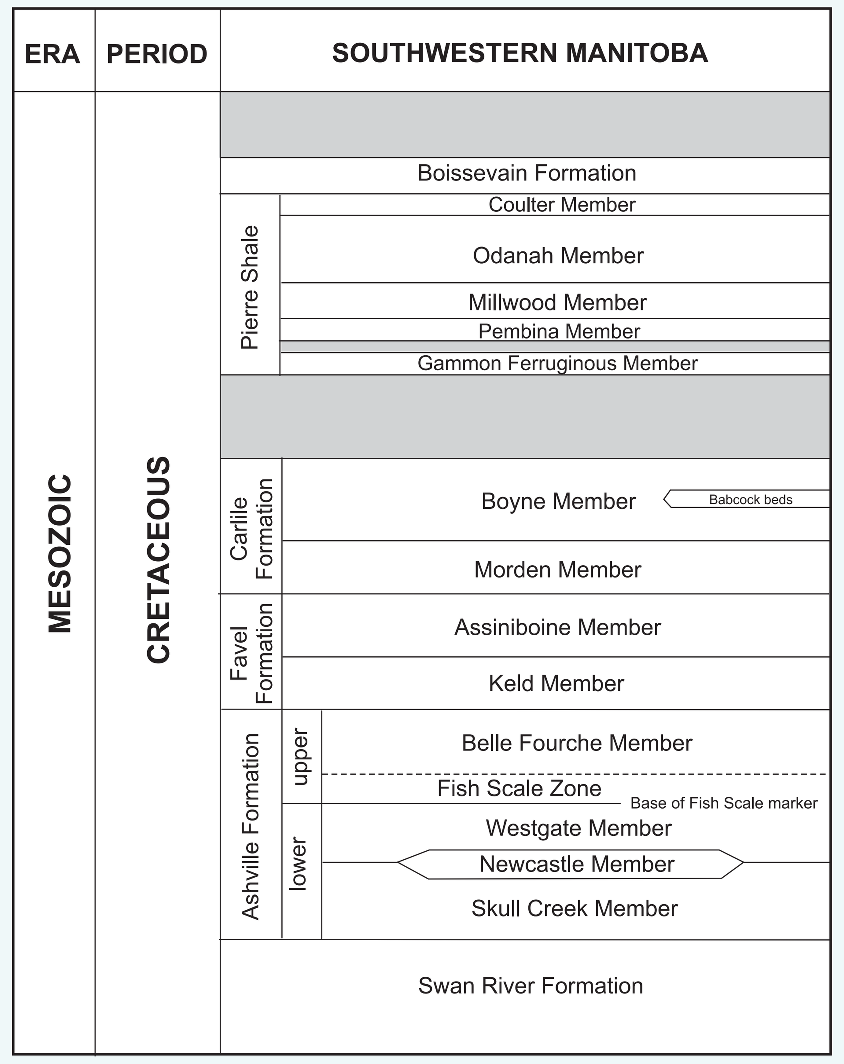

Figure 2: Cretaceous stratigraphy of southwestern Manitoba (Nicolas and Bamburak, 2011).

Chemostratigraphy

The Gammon Ferruginous has high total organic carbon (TOC) values indicating its capacity to act as very good source rocks for hydrocarbons. RockEval™ 6 analysis returned Tmax values for all the samples below the oil window of 435°C, which is needed to reach thermal maturation; such low values are expected due to its shallow burial history (Figure 3).

X-ray diffraction (XRD) was conducted on drill cuttings to determine bulk mineralogy. The average mineral abundances are shown in Figure 4. The dominant phases in the Gammon Ferruginous member are illite and quartz with minor phases of pyrite and plagioclase with trace amounts of chlorite and siderite.

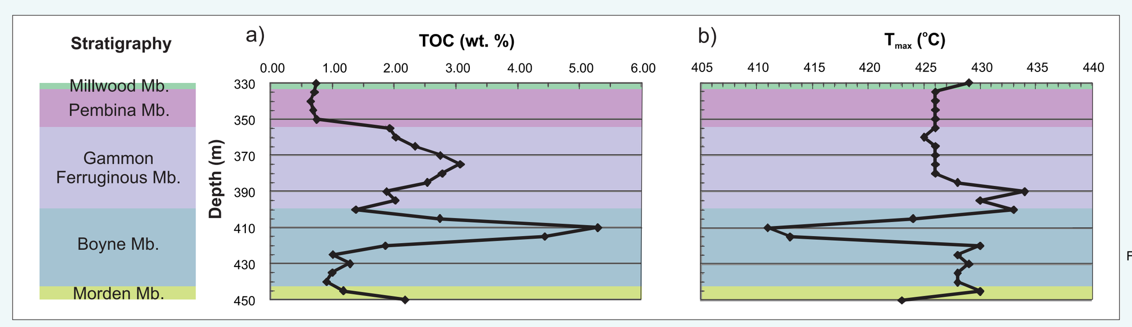

Figure 3: RockEval and total organic carbon data grouped by member and placed in order of stratigraphic depth: a) total organic carbon (TOC) and b) temperature at maximum release of hydrocarbons (Tmax) depth profile of the drill-cutting samples from the Relative Daly Sinclair HZNTL 8-31-7-29W1 well (L.S. 8, Sec. 31, Twp. 7, Rge. 29, W 1st Mer., southwestern Manitoba); sample interval is 5 m (Nicolas and Bamburak, 2012).

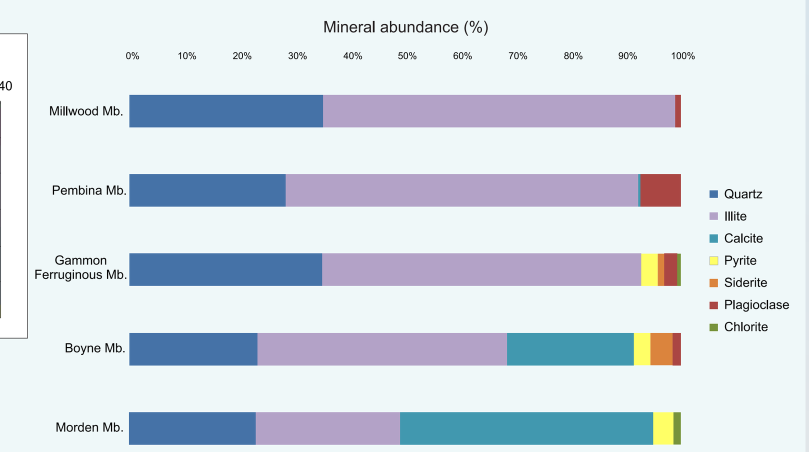

Figure 4: Average mineral abundance of Cretaceous drill cuttings from the Relative Daly Sinclair HZNTL 8-31-7-29W1 well as determined by X-ray diffraction (Nicolas and Bamburak, 2012).

The Gammon Ferruginous Member shows potential as a shale gas reservoir in Manitoba. Its commonly shaly silt to sand lithology, natural fracture network, high organic content and consistently high Pason™ gas readings are common features of shale gas reservoirs. Its variations in thickness over short distances can provide stratigraphic and hydrological trapping mechanisms to create localized gas accumulations (sweet spots) in an otherwise continuous reservoir. Sweet spots and pool boundaries defined by economic limits are common in shale gas plays, such as the equivalent Milk River Formation play in southwestern Saskatchewan. The Milk River Formation giant gas fields are prolific and long-lived gas-producing plays, which can be used as an analogue for the potential shale gas play that may exist in Manitoba. In the extreme southwestern corner of Manitoba, the Gammon Ferruginous Member occurs at maximum depths of approximately 450 m, which is on par with the producing depths of the Milk River Formation (O'Connell, 2003).

Chemostratigraphy (continued)

During the summer of 2010, four new localities with Gammon Ferruginous Member were found and sampled and six localities were resampled (Table 1). Preliminary results from 25 samples sent for INAA and ICPES inorganic chemical analyses showed that the Spencer's ditch has the highest values for most REE and Th, U and P (Table 1) relative to all other Cretaceous shale analyses in the chemostratigraphic database. Similarly, the Holo Crossing has the highest values for Yb, Lu, Ni and Zn (Table 1), while the Mount Nebo has the highest Cu and V (Table 1).

Table 1: Gammon Ferruginous Member analytical results (after Bamburak and Nicolas, 2010)

	Th (ppm)	U (ppm)	La (ppm)	Ce (ppm)	Nd (ppm)	Sm (ppm)	Eu (ppm)	Tb (ppm)	Yb (ppm)	Lu (ppm)	Y (ppm)	Cu (ppm)	Ni (ppm)	V (ppm)	Zn (ppm)	Fe (%)	P (%)
Detection limit	0.2	0.5	0.5	3	5	0.1	0.2	0.5	0.2	0.05	1	1	1	2	1	0.01	0.001
Analysis method	INAA	INAA	INAA	INAA	INAA	INAA	INAA	INAA	INAA	INAA	TD-ICP	TD-ICP	MULT	TD-ICP	MULT	INAA	TD-ICP
1996-2007 sample analyses - Pembina Hills area																	
Average of 11 outcrop	15.2	73.8	170.1	228	128	2.5	7.5	5.3	18.6	3.08	319	96	115	641	230	8.69	1.307
Maximum values of above sample analyses	41.0	230.0	760.0	900	580	110.0	34.4	27.0	79.6	13.50	1656	159	180	1137	401	27.70	5.351
2010 sample analyses - several localities																	
Maximum value from several localities	45.4	244.0	904.0	934	627	129.0	37.8	23.1	101.0	16.90	>1000	202	1290	1350	2800	14.0	5.430

Abbreviations: INAA, instrumental neutron activation analyses; MULT, multi-element instrumental neutron activation analysis; TD-ICP, inductively coupled plasma-emission spectrometry with total digestion.

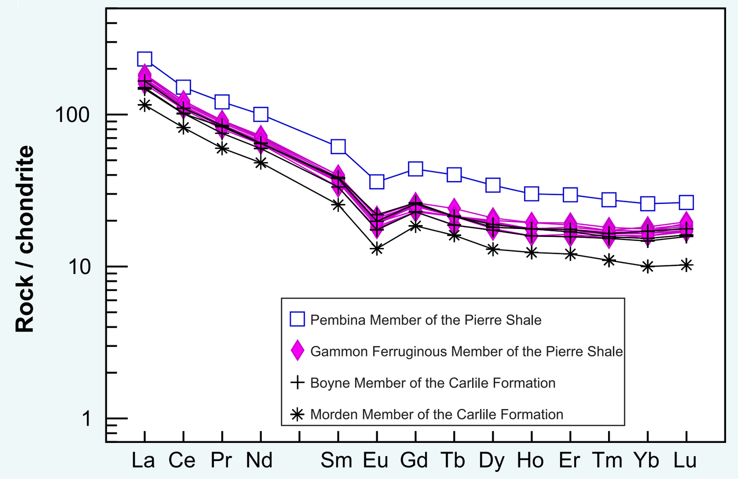

Figure 5: Chondrite-normalized rare earth element (REE) diagram for washed drill-cutting samples from Relative Daly Sinclair HZNTL 8-31-7-29W1 well (Bamburak et al., 2012).

Figure 6: In the shale-normalised plot (after Taylor & McLennan, 1958) it is possible to see a middle REE-(MREE) enriched pattern suggesting strongly diagenetic bioapatite (C. Trueman, personal communication, 2014).

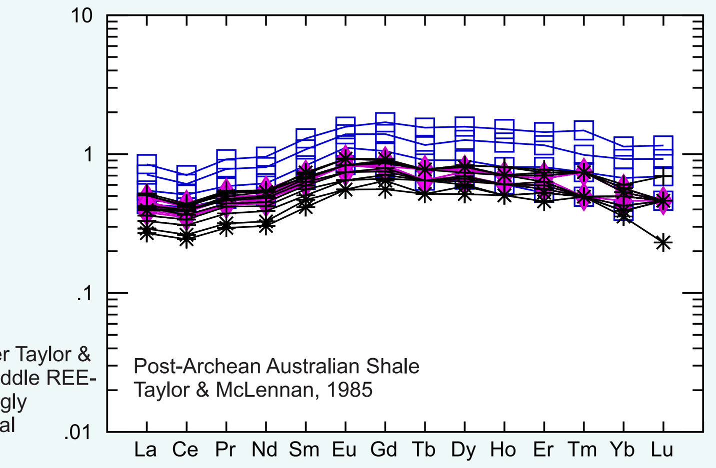

Electron microprobe analyses

The main objective of electron-probe microanalyses, carried out at the University of Manitoba, was to understand if the apatite (contained in sample 99-12-SD-002B from Spencer's ditch, Figure 1) identified by the Saskatchewan Research Council (SRC) is the principal carrier of the REE, as previously suggested by Bamburak et al. (2013). In an initial stage of this study, round mounts prepared and analyzed by the SRC were re-used in order to ensure that analytical results were obtained from the same mineral grains. However, the analyses performed on these mounts produced low sum totals (Martins et al., 2014), this may be as a result of the grains being damaged by the electron beam in the initial analysis. This damage may have resulted from a number of factors, such as a defocusing effect, beam-sensitive samples, type of epoxy used in the round mounts or low connectivity related to the nature of the mounts (when compared to a thin section). In order to mitigate the analytical problems described above new mounts were prepared for this study.

All values and characteristics of the apatite grains presented in this poster refer to the results obtained from thin sections only. The data obtained for round mineral mounts are available in Martins et al. (2014), but are not discussed here due to poor quality of the electron-probe data resulting from extensive beam damage to the samples.

Observations under the polarizing microscope were compromised due to the variable thickness of the thin sections. Nevertheless, it is possible to observe that the grains are subhedral to anhedral, usually appear cloudy or with inclusions of different materials or porosity. BSE imagery also allows to observe primary porosity (Figure 7).

The apatite grains vary in size from 80 to 250 µm in the mesh size 100–250, and from 150 to 400 µm in the 250–300 mesh. The BSE imagery and X-ray maps indicate that most the apatite grains have little to no zoning (Figure 8 and 9).

All of the oxide totals are low, with a highest total of 97.80 wt. % and a lowest of 72.77 wt. % (Table 2; Martins et al., 2014, Table 2).

The highest total of rare-earth element oxides ranges from 0.50 to 2.11 wt. % (Martins et al., 2014, Table 2). The FeO content is quite high in some of the analyzed grains (up to 11.82 wt. %) and SO_3 content varies from 1.10 to 2.20 wt. % (Martins et al., 2014).

Table 2: Selected results of electron microprobe analyses of studied apatite grains.

Oxides (wt. %)	Sample number						
	S1-Ap1_C	S1-Ap3_C	S1-Ap7_C	S2-Ap2_C	S2-Ap3_C	S2-Ap4_C	S2-Ap9_C
Na_2O	1.12	1.14	1.35	1.23	1.07	0.95	1.12
Al_2O_3	0.66	2.17	1.04	2.27	1.56	0.54	2.66
SiO_2	0.02	0.04	0.02	0.00	0.05	0.00	0.02
P_2O_5	35.77	36.24	36.53	36.68	34.93	35.64	35.46
SO_3	2.20	1.77	1.75	1.27	1.35	2.17	1.67
CaO	50.92	49.01	34.35	43.97	47.34	50.69	48.69
FeO	0.93	1.34	11.82	3.41	0.85	0.78	0.80
MnO	0.07	0.17	0.05	0.13	0.15	0.10	0.18
SrO	0.27	0.33	0.19	0.24	0.26	0.25	0.27
BaO	0.07	0.08	0.17	0.24	0.08	0.04	0.13
La_2O_3	0.14	0.17	0.32	0.52	0.32	0.10	0.13
Ce_2O_3	0.19	0.00	0.40	0.59	0.47	0.25	0.00
Pr_2O_3	0.19	0.19	0.22	0.10	0.00	0.00	0.25
Nd_2O_3	0.02	0.00	0.60	0.42	0.34	0.17	0.27
Sm_2O_3	0.17	0.03	0.17	0.00	0.03	0.20	0.10
Dy_2O_3	0.18	0.23	0.00	0.08	0.12	0.00	0.01
Y_2O_3	0.13	0.27	0.47	0.80	0.52	0.22	0.18
F	3.94	4.62	2.39	3.67	4.38	3.89	4.92
Total	96.99	97.80	91.84	95.62	93.82	95.99	96.86
ΣREEO+Y_2O_3	1.02	0.89	2.18	2.51	1.80	0.94	0.94

Notes: Cl was sought but it was below detection limit. Abbreviations: C, core of apatite; REEO, rare-earth element oxides; S1, thin section 1 with 100–250 mesh; S2, thin section 2 with 250–300 mesh.

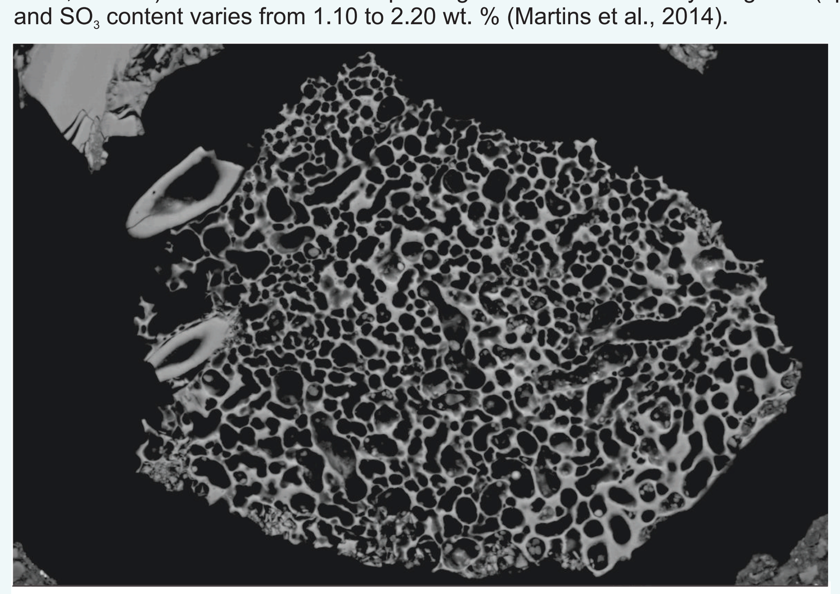

Figure 7: BSE imagery of apatite grain from the Gammon Ferruginous Member showing evidence of primary porosity (Bamburak et al., 2014).

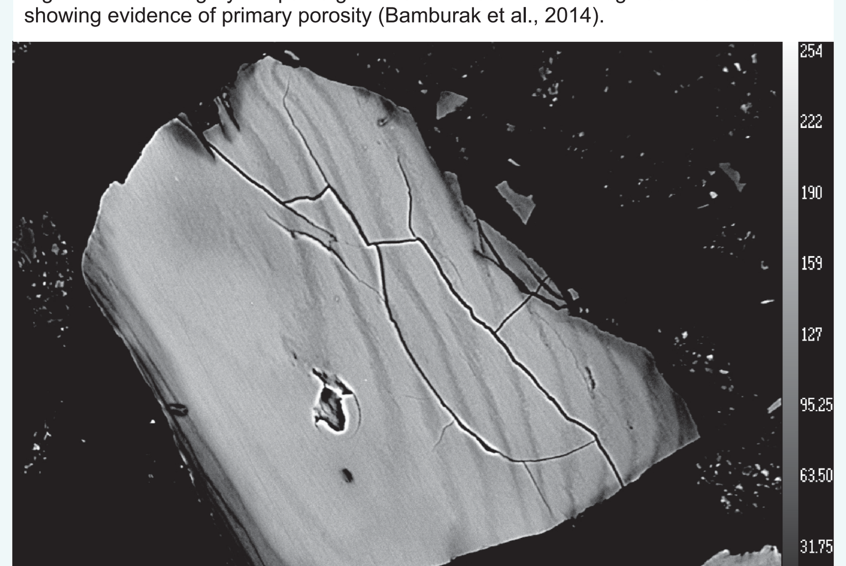

Figure 8: BSE image of a grain approximately 200 microns with apparent chemical zoning (possibly petrified wood) (Bamburak et al., 2014).

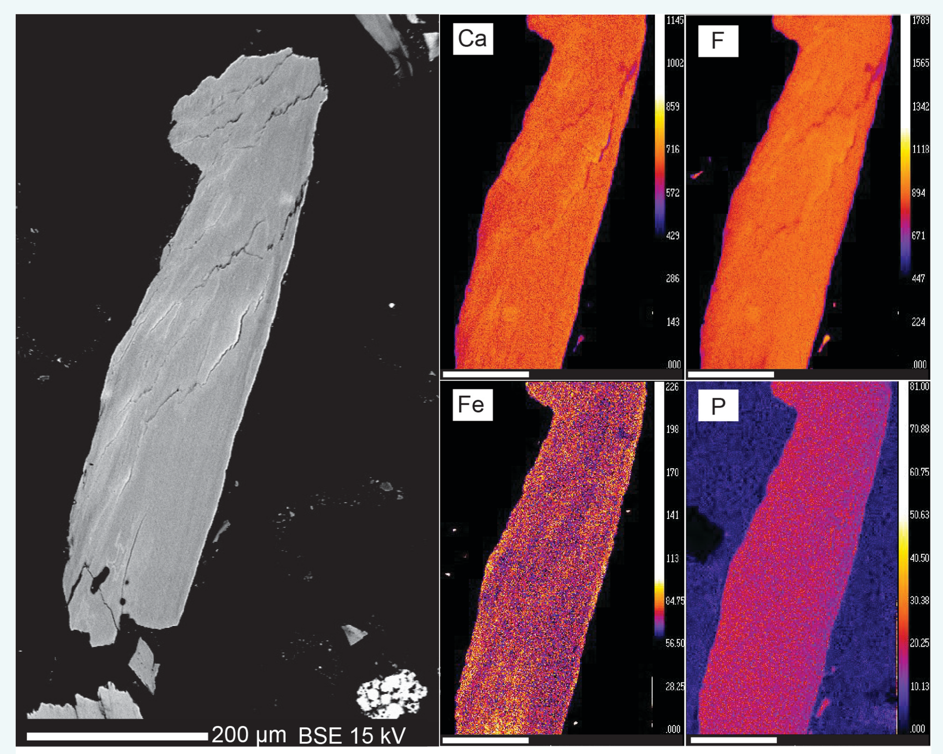

Figure 9: BSE image of apatite grain with X-ray maps; insets of the same grain showing no significant internal variation for elements Ca, F, Fe and P (scale bar insets are 100 µm) (Bamburak et al., 2014).

Paleontology

The Spencer's ditch outcrop of the Gammon Ferruginous Member in Manitoba is the second thickest outcrop of this member in the Manitoba escarpment (Bamburak and Nicolas, 2010) and continues to produce vertebrate fossils of tremendous paleontological significance. The sand grains within the lower and middle units of the Gammon Ferruginous Member tend to be angular, indicating that they have not traveled far from their erosional source. Furthermore, the abnormal concentration of flightless bird fossils preserved in the *Xiphactinus* Kill Zone quarry (Figure 10 and 11) could also allude to a reasonably nearshore environment of deposition.

Nicholls (1988) first noted the concentration of fossil birds at this locality in 1988, along with a comparatively lower number of larger marine reptile skeletons. Nicholls (1988) hypothesized that Spencer's ditch may have represented a sheltered area particularly abundant in birds, where mosasaurs and plesiosaurs did not frequently congregate.

Recent palynology analysis of the bentonite layers sampled by the Canadian Fossil Discovery Centre (CFDC) from the lower unit of the Gammon Ferruginous Member at this locality has identified terrestrially derived conifer pollens *Bisaccate* and *Classopollis classoides*. Of these two conifer pollens, *C. classoides* is known to have occupied well-drained soils of upland slopes and lowlands near coastal areas, preferring the warm climate of transgressive seas (Srivastava, 1976). The presence of *C. classoides* in the lower unit of the Gammon Ferruginous Member is consistent with McNeil and Caldwell's (1981) interpretation that the earliest sediments of the transgressive Pierre Sea developed incisions into the lower surfaces of the Boyne Sea, and successively overstepped the previously deposited chalky unit of the Boyne Member (McNeil and Caldwell, 1981).

Conifer pollens have been well documented in nearshore terrestrial ecosystems of North America in Cretaceous time, including fluvial deposition along lowland coastal plains directly into the Western Interior Seaway (Hatcher, 2006).

Figure 10: CFDC fossil crew in the *Xiphactinus* Kill Zone quarry (Bamburak et al., 2012).

Figure 11: View of a bone bed in the *Xiphactinus* Kill Zone quarry within the middle Gammon Ferruginous Member at Spencer's ditch (two rib bones are ~4 cm) (Bamburak et al. 2012).

Discussion

The results from the electron microprobe analyses do not allow calculation of the chemical formulas from the mineral analyses using the ideal formula for fluorapatite: $Ca_5(PO_4)_3F$. The extent of the damage caused in some of the grains is very unusual for magmatic apatite further more, textural evidence of primary porosity is observed under the optical microscope and in BSE imagery (Figure 7), which is not commonly observed in magmatic apatite.

Taking these aspects into account as well as observations from shale normalised plot (Figure 5), the apatite recovered from the Gammon Ferruginous Member is interpreted to be biological apatite, representing fossil bone rather than magmatic apatite.

In biological systems, calcium orthophosphates occur as the principal inorganic constituent of bones, teeth, fish enameloid and some species of shells, as well as pathological calcifications (e.g., dental and urinary calculus and stones, atherosclerotic lesions). Structurally, they occur mainly in the form of poorly crystallized nonstoichiometric sodium-, magnesium- and carbonate-containing carbonated hydroxyapatite (often called biological apatite or dahllite).

The literature provides many examples of highly enriched REE in fossilized bone or bone beds. For example, the Pleistocene Olorgesailie Formation of southern Kenya has total REE concentrations in fossil bones ranging from 33 to 48 175 ppm (Trueman et al., 2006). Another example is the Monte San Giorgio beds at Ticino, Switzerland (240 Ma), where the Meride Formation has an average total REE concentration of 2200 ppm and the Besano Formation has variable REE contents, from very low (300–800 ppm) to very high (>10 000 ppm; Kocsis et al., 2010). Although most trace elements are probably only adsorbed onto the surface of fossil bones (e.g., Shaw and Wasserburg, 1985), it is observed that these concentrations may increase significantly (up to thousands of ppm) in fresh bones and teeth during diagenesis. These authors attribute the increase in REE to the diffusion and adsorption onto crystallite surfaces, possibly during transformation of bone material, and state that the increase in trace-element content is unequivocally diagenetic in origin (Trueman, 2007).

Taking all of this into consideration, the concentrations of rare-earth element oxides in the Gammon Ferruginous Member are comparable to examples from elsewhere in the literature (as indicated above) and could be explained by biological apatite, which contains up to 2.96 wt. % of rare-earth element oxides plus Y_2O_3 in the present case.

Economic considerations:

The origin of the REE mineralization within the Gammon Ferruginous Member of the Pierre Shale seems to be associated with the bone beds and at the present time the origin of the REE fluid that caused this enrichment is uncertain. However, systematic testing of Cretaceous stratigraphic units, using portable XRF units to detect anomalous concentrations of REE, might be a useful tool to find bone beds, which might yield significant fossil finds of marine reptiles, such as the mosasaurs and plesiosaurs on display at the CFDC in Morden. The significant fossil discoveries that can occur using this methodology would further enhance the recognition of the CFDC in the scientific community and on the world stage. Greater recognition can directly result in more successful funding requests by the CFDC to expand its museum and services, attraction of world-class scientists and technical people to work and live in the local community, and help grow the centre as a major must-see attraction in Manitoba. All of these have direct economic benefits to the local community, and to Manitoba as a whole.

Although the original purpose of this project, begun several years ago, was to describe the potential for economic REE mineralization within the Gammon Ferruginous Member of the Pierre Shale, the determination that REE seem to have only accumulated in the bones of Cretaceous creatures reduces the possibility of making an economic discovery. However, to confirm or reject this hypothesis, additional analytical testing will be done on the outcrop samples collected in 2014 in the Vermilion River area.

References

Bamburak, J.D. & Nicolas, M.P.B. 2009: Geoscientific Presentation PRES2009-25.
Bamburak, J.D. & Nicolas, M.P.B. 2010: Report of Activities, Manitoba Innovation, Energy and Mines, MGS, p. 170–177.
Bamburak, J.D. et al. 2012: Report of Activities, Manitoba Innovation, Energy and Mines, MGS, p. 141–150.
Bamburak, J.D. et al. 2013: Report of Activities, Manitoba Mineral Resources, MGS, p. 123–128.
Bamburak, J.D. et al. 2014: Report of Activities, Manitoba Mineral Resources, MGS.
Bannatyne, B.B. 1970: Department of Mines and Natural Resources, Mines Branch, Publication 67-1, 107p.
Christopher, J.E. & Yurkowski, M. 2007: Report 2007-4.1, CD-ROM, Paper A-9, 18 p.
Kocsis, L. et al. 2010: Geochimica et Cosmochimica Acta, v. 74, no. 21, p. 6077–6092.
Hatcher, J. 2006: P.M. Natural History Museum, London, United Kingdom, p. 52–54.
Martins, T. et al. 2014: DRI- suplementary material.
McNeil, D.H. & Caldwell, W.G.E. 1981: GAC, Special Paper no. 21, 439p.
Nicholls, E.L. 1988: Ph.D. thesis, University of Calgary, Calgary, Alberta, 317 p.
Nicolas, M.P.B. 2009: Geoscientific Paper GP2009-1,19 p.
Nicolas, M.P.B. & Bamburak, J.D. 2011: Report of Activities, Manitoba Innovation, Energy and Mines, MGS, p. 143-149.
Nicolas, M.P.B. & Bamburak, J.D. 2012: Report of Activities, Manitoba Innovation, Energy and Mines, MGS, p. 134–140.
O'Connell, S. 2003: Belfield Resources Inc., Calgary, Alberta, 247 p.
Taylor, S.T. & McLennan S. M. (1985): Blackwell Scientific Publications, 312 p.
Trueman, C. 2007: The University of Chicago Press, Chicago and London, p. 397–435.
Trueman, C.N. et al. 2006: Geochimica et Cosmochimica Acta, v. 70, p. 4343–4355.
Shaw, H. & Wasserburg, G. 1985: Geochimica et Cosmochimica Acta, v. 49, p. 503–518.
Srivastava, S.K. 1976: Lethaia, v. 9, no. 4, p.437–457.
Sun, S. & McDonough, W.1989: Geological Society, Special Publication 42, p. 313–345.

Acknowledgments

R. Unruh is thanked for his patience in preparing the thin sections for this report. R. Sidhu is acknowledged for her help acquiring electron-probe microanalyses data and resolving analytical problems. The authors would also like to thank J. Harrison (University of Manitoba) for providing her enthusiastic assistance in sampling of the Vermilion River outcrops.